Molecular Crystals and Liquid Crystals

ISSN: 1542-1406 (Print) 1563-5287 (Online) Journal homepage: http://www.tandfonline.com/loi/gmcl20

# Studies of an Intermolecular Hydrogen-Bonded Complex of Butyloxy Benzoic Acid and Dipyridyl Ethylene

**Ambika Sambyal, Gurpreet Kour, Shivangi Sharma, Rajinder K. Bamezai, Sumati Anthal, Vivek K. Gupta, Rajni Kant & C. V. Yelamaggad**

**To cite this article:** Ambika Sambyal, Gurpreet Kour, Shivangi Sharma, Rajinder K. Bamezai, Sumati Anthal, Vivek K. Gupta, Rajni Kant & C. V. Yelamaggad (2015) Studies of an Intermolecular Hydrogen-Bonded Complex of Butyloxy Benzoic Acid and Dipyridyl Ethylene, Molecular Crystals and Liquid Crystals, 608:1, 135-145, DOI: 10.1080/15421406.2014.953745

**To link to this article:** http://dx.doi.org/10.1080/15421406.2014.953745

Published online: 03 Mar 2015.

*Mol. Cryst. Liq. Cryst.*, Vol. 608: pp. 135–145, 2015

ISSN: 1542-1406 print/1563-5287 online
DOI: 10.1080/15421406.2014.953745

Taylor & Francis
Taylor & Francis Group



# Studies of an Intermolecular Hydrogen-Bonded Complex of Butyloxy Benzoic Acid and Dipyridyl Ethylene

AMBIKA SAMBYAL,[1] GURPREET KOUR,[1] SHIVANGI SHARMA,[1] RAJINDER K. BAMEZAI,[1,*] SUMATI ANTHAL,[2] VIVEK K. GUPTA,[2] RAJNI KANT,[2] AND C. V. YELAMAGGAD[3]

[1]Department of Chemistry, University of Jammu, Jammu, India
[2]Department of Physics, University of Jammu, Jammu, India
[3]Centre for Soft Matter Research, Jalahalli, Bengaluru, India

*A symmetric hydrogen-bonded liquid crystalline complex was synthesized from 4-n-butyloxy benzoic acid and 1,2-di-(4-pyridyl)-ethylene. The complex was analyzed by optical polarizing microscopy, differential scanning calorimetery, and thermal gravimetric analysis. The existence of hydrogen-bonding for the complex was confirmed by Fourier transform infrared spectroscopy and x-ray crystallography. The liquid crystalline complex crystallizes with a triclinic space group P1with the parameters* $a = 7.3331(4)$ *Å,* $b = 9.0701(4)$ *Å,* $c = 11.6957(5)$ *Å and* $\alpha = 81.896(4)^\circ$, $\beta = 79.239(4)^\circ$, *and* $\gamma = 85.652(4)^\circ$.

**Keywords** Hydrogen bonding; smectic A phase; p-*n*-alkoxy benzoic acid; phase transition

## 1. Introduction

Liquid crystalline materials, also known as functional materials, are known for their stability, directionality, and dynamic nature due to their alignment in presence of external fields like magnetic or electric field. This leads to their applications in display devices. In addition to it, new properties can arise from ordering the liquid crystalline materials through noncovalent interactions. In particular, the use of hydrogen bond, as a noncovalent interaction, can be an important tool in construction and ordering of mesogenic materials which has now gained much importance in many areas of chemical and biological processes, such as, molecular recognition and self-assembly [1]. Hydrogen bond interactions are stronger than van der Waals interactions [2]; they can bring about a self-assembly of supramolecular aggregates [3, 4]. In recent years, much attention has been paid to the development of several supramolecular mesogenic materials via molecular self assembly through hydrogen bonding [5–12]. Earlier, Bradfield et al. [13] and Gray

*Address correspondence to Rajinder K. Bamezai, Department of Chemistry, University of Jammu, Jammu 180006, India. E-mail: rkb10@rediffmail.com

Color versions of one or more of the figures in the article can be found online at www.tandfonline.com/gmcl.

and Jones [14] found that hydrogen bonding in 4-substituted benzoic acids can induce the formation of liquid crystalline phases. However, their study was restricted to single component systems. Kato and Frechet [15] were the first to demonstrate that hydrogen bonding between carboxylic group and pyridyl moieties was useful for the formation of supramolecular hydrogen-bonded associates. Subsequently, in most of the reported hydrogen bonded complexes, 4-alkyl benzoic acids and 4-alkoxy benzoic acids have been widely used as potential proton donors, whereas 4,4′-bipyridine has been used as potential proton acceptor. Since scanty information on the liquid crystal behavior of the hydrogen bonded liquid crystals derived from 1,2-di-(4-pyridyl)-ethylene is available in the literature [16, 17], the present investigation was carried out. Herein, we describe the phase behavior of hydrogen-bonded liquid crystalline complex obtained from 4-*n*-butyloxy benzoic acid and 1,2-di-(4-pyridyl)-ethylene. The presence of hydrogen bond in this complex was verified by FTIR and X-ray diffraction studies and the liquid crystalline properties were established through polarizing optical microscope, differential scanning calorimeter, and thermal analysis.



## 2. Materials and Methods

All chemicals were commercially available from Sigma Aldrich (analar grade) and used without further purification. The intermolecular hydrogen bonded complex (**3**) was synthesized by stirring 4-butyloxy benzoic acid (**1**) (BOBA: 0.30 mmoles) and 1, 2-di-(4-pyridyl)-ethylene (**2**) (DPE: 0.30 mmoles) in dry dimethyl formamide (DMF), at room temperature, for about 24 hr. The mixture was left as such for 12 hr. A colorless compound was obtained by slow evaporation of the DMF solution at room temperature, followed by drying under vacuum. The yield of the complex was 90%.

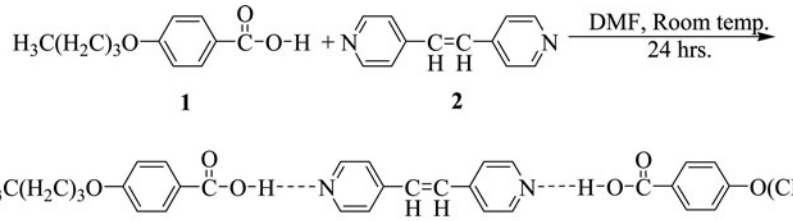


The optical textures were observed using Leitz polarizing microscope (POM) with Mettler hot stage. The IR spectrum was recorded on Perkin Elmer FTIR spectrophotometer. The differential scanning curves (DSC) were obtained using Perkin Elmer instrument, while the thermal analysis (TA) results, namely, differential thermal analysis and thermal gravimetric analysis (DTA and TGA), were obtained from Linesis thermal analyzer using a scanning rate of 5°C $min^{-1}$ in each case.

The x-ray intensity data of 25703 reflections (5871 being unique ones) of the crystals were collected at 293 K using X'calibur CCD area-detector diffractometer (Oxford diffraction make, UK) equipped with graphite monochromatic Mo$K\alpha$ radiation ($\lambda = 0.71073$ Å) operating at 50 kV and 30 mA. The structure was solved by direct methods and successive difference map (SHELXS-97) and refined by full-matrix least-square F2 using all unique data (SHELXL-97) [18]. The crystal used for data collection was of dimensions 0.3 × 0.2 × 0.2 $mm^3$.

**Plate 1.** Marbled textures of nematic phase at 175.0°C.

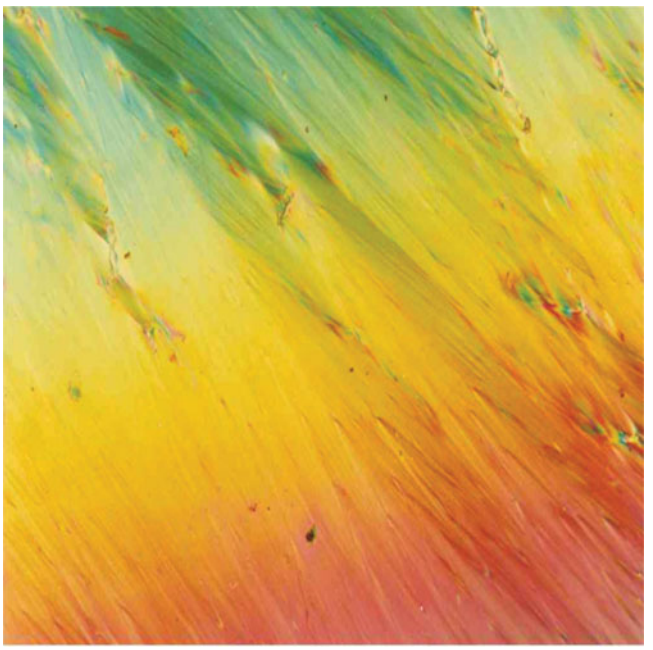

**Plate 2.** Focal conic fan-shaped textures of smectic A phase at 160.0°C.

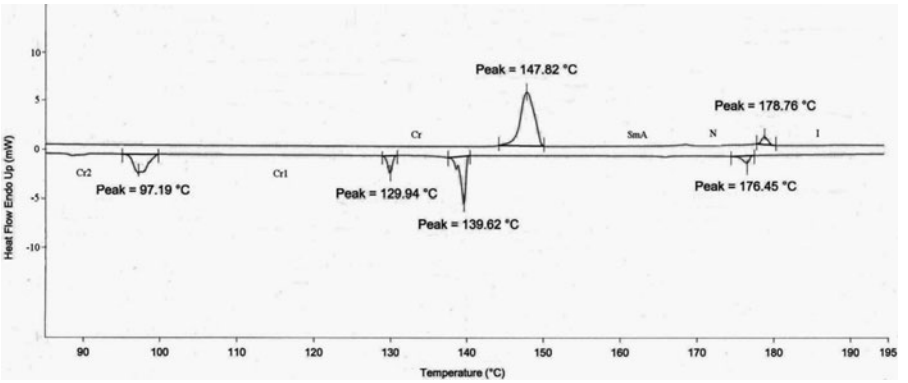


**Figure 1.** Differential scanning curve of complex obtained upon heating and cooling at the rate of 5°C $min^{-1}$.

## 3. Results and Discussion

### *3.1. POM, DSC, and TA Studies*

DPE (**2**) is nonmesomorphic which melts directly to isotropic liquid at 152°C, while BOBA (**1**) shows a nematic phase in the range from 147–160°C. The mesomorphic behavior of the complex **(3)** was studied using POM, DSC, and TA studies. The POM studies, on heating, revealed textures [19] similar to smectic A phase at 147.8°C which then changed

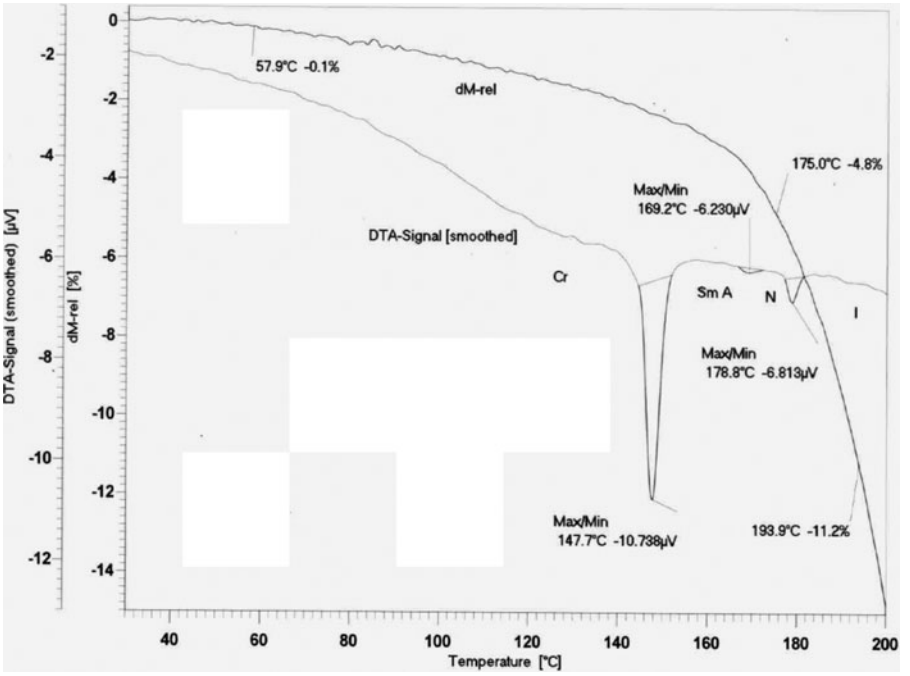


**Figure 2.** DTA and TGA curves of the complex obtained upon heating only at the rate of 5°C $min^{-1}$.

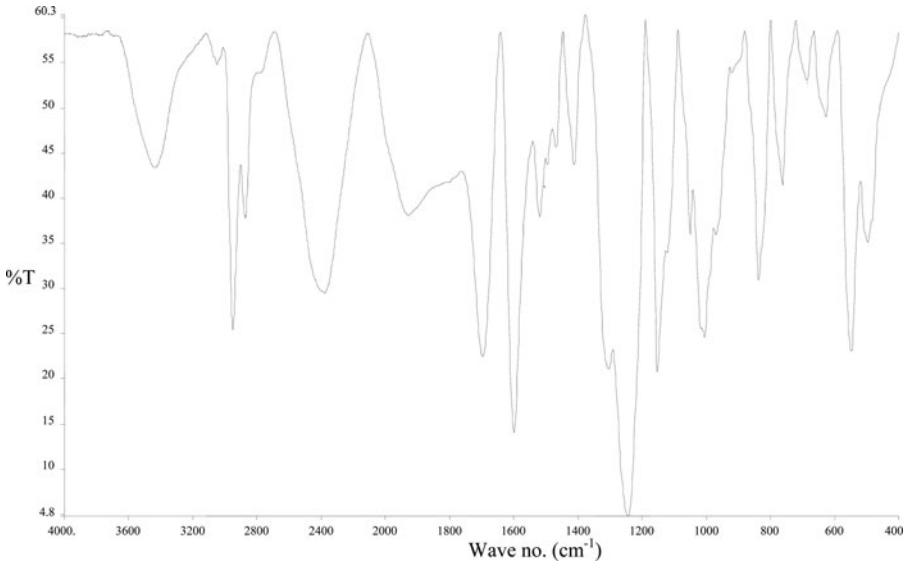


**Figure 3.** FTIR spectra of the complex.

to nematic phase at about 171.0°C followed by transition into the isotropic state at 178.8°C. During cooling, the nematic marbled textures (Plate 1) appeared which at lower temperature converted into focal conic fan shaped textures (Plate 2).

The phase transition temperature observed through POM is found to be enantiotropic one and in agreement with DSC (Fig. 1). The thermogram in the heating cycle shows two well-defined endothermic peaks at 147.8°C and 178.7°C with enthalpy change values as 97.12 and 6.05 $Jg^{-1}$, respectively. These two peaks correspond to the crystal to smectic A and nematic to isotropic phase transitions. The transition from smectic A to nematic phase is accompanied with very small change in heat flow at about 170.0°C, and hence the enthalpy change could not be evaluated in the heating or in the cooling mode. In the subsequent cooling cycle, there were four exothermic peaks possessing the transitions, namely, isotropic to nematic, smectic A to crystal followed by two crystal to crystal changes at 176.45°C, 139.62°C, 129.94°C, and 97.19°C, respectively; the corresponding enthalpy values being 6.82, 33.91, 10.68, and 34.04 $Jg^{-1}$.

The DSC scan agreed well with the data obtained from DTA (Fig. 2). The interesting feature of DTA is that the transition from smectic A to nematic phase was resolved in this

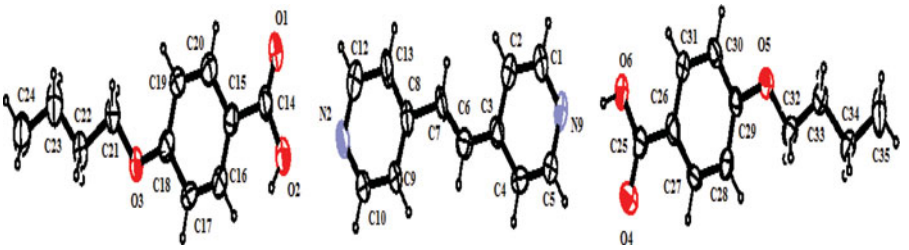


**Figure 4.** ORTEP view of the complex. Hydrogen atoms are shown as small spheres of arbitrary radii.

**Table 1.** Crystal data and other experimental details

| CCDC no. | 963048 |
|---|---|
| Chemical formula | $C_{34}\ H_{38}N_2O_6$ |
| Crystal description | Block shaped |
| Crystal color | White |
| Crystal size | $0.3 \times 0.2 \times 0.2$ mm$^3$ |
| Formula weight | 570.66 |
| Crystal system | Triclinic |
| Space group | P1 |
| Unit cell volume | 755.61(6) |
| No. of molecules per unit cell, $Z$ | 2 |
| Unit cell dimensions | $a = 7.3331(4)$, $b = 9.0701(4)$, $c = 11.6957(5)$ [Å] $\alpha = 81.896(4)^\circ$, $\beta = 79.239(4)^\circ$, $\gamma = 85.652(4)^\circ$ |
| $d_c$, g cm$^{-3}$ | 1.254 |
| Temperature | 293(2) |
| Absorption coefficient | 0.086 mm$^{-1}$ |
| F(000) | 304 |
| Scan mode | $\omega$ scan |
| $\theta$ Range for entire data collection | $3.54 < \theta < 26.00^\circ$ |
| Range of indices | $h = -9$ to 9, $k = -11$ to 11, $l = -14$ to 14 |
| Reflections collected/unique | 25703 / 5871 |
| No. of parameters refined | 381 |
| Reflections observed ($I > 2\sigma(I)$) | 3501 |
| $R_{int}$ | 0.0529 |
| $R_{sigma}$ | 0.0479 |
| Final $R$ | 0.0532 |
| $wR(F^2)$ | 0.1317 |
| Goodness-of-fit | 0.980 |
| $(\Delta/\sigma)_{max}$ | 0.208e Å$^{-3}$ |
| Final residual electron density | $-0.187 < \Delta\rho < 0.208$e Å$^{-3}$ |



case and the peak temperature observed were 147.7°C (Cr to Sm A; $\Delta H = 86.83$ Jg$^{-1}$, $\Delta C_p = 0.82$ Jg$^{-1}$K$^{-1}$), 169.2°C (Sm A–N; $\Delta H = 0.42$ Jg$^{-1}$, $\Delta C_p = 0.54$ Jg$^{-1}$K$^{-1}$), and 178.8°C (N–I; $\Delta H = 6.97$ Jg$^{-1}$, $\Delta C_p = 0.39$ Jg$^{-1}$K$^{-1}$). Thus, the transition temperature and change in enthalpy parameters evaluated from DSC and DTA techniques agreed well with each other.

Simultaneously, the stability of the complex was also viewed through TGA studies, depicted in Fig. 2, as change in relative mass [dM-rel,%] versus function of temperature. The TGA curve reveals the hydrogen bonded complex to be quite stable in going from room temperature to the isotropic change; the total weight loss being only 4.8% till 175.0°C, that is, very near to the isotropic state followed by a rapid loss of 11.2% till 193.9°C.

**Table 2.** Atomic coordinates and equivalent isotropic thermal parameter (Å$^2$) for non-hydrogen atoms (e.s.d's are given in parentheses)

| Atom | *x* | *Y* | *z* | $u_{eq}$* |
|---|---|---|---|---|
| C1 | 1.1682(10) | −0.2637(7) | 0.4474(7) | 0.074(2) |
| C2 | 1.0931(9) | −0.1173(6) | 0.4590(6) | 0.0643(18) |
| C3 | 1.0963(8) | −0.0621(6) | 0.5633(5) | 0.0540(16) |
| C4 | 1.1709(9) | −0.1516(5) | 0.6461(5) | 0.0581(17) |
| C5 | 1.2440(10) | −0.2930(6) | 0.6268(6) | 0.0643(18) |
| C6 | 1.0152(8) | 0.0921(5) | 0.5735(6) | 0.0534(15) |
| C7 | 0.9929(9) | 0.1580(6) | 0.6689(6) | 0.0569(17) |
| C8 | 0.9197(8) | 0.3072(5) | 0.6843(5) | 0.0468(14) |
| C9 | 0.9194(8) | 0.3700(6) | 0.7848(5) | 0.0570(16) |
| C10 | 0.8496(9) | 0.5099(6) | 0.7967(5) | 0.0590(16) |
| C12 | 0.7701(10) | 0.5392(6) | 0.6155(6) | 0.0701(18) |
| C13 | 0.8407(10) | 0.3986(6) | 0.5963(6) | 0.0721(19) |
| C14 | 0.6522(8) | 0.9099(6) | 0.8475(5) | 0.0517(15) |
| C15 | 0.5659(8) | 1.0591(5) | 0.8632(5) | 0.0445(14) |
| C16 | 0.5842(8) | 1.1276(5) | 0.9564(5) | 0.0505(14) |
| C17 | 0.5023(8) | 1.2697(5) | 0.9715(5) | 0.0523(14) |
| C18 | 0.4092(8) | 1.3437(5) | 0.8886(5) | 0.0495(14) |
| C19 | 0.3890(8) | 1.2810(5) | 0.7940(5) | 0.0507(14) |
| C20 | 0.4692(8) | 1.1334(6) | 0.7807(5) | 0.0503(15) |
| C21 | 0.3371(9) | 1.5637(6) | 0.9881(5) | 0.0563(16) |
| C22 | 0.2267(9) | 1.7068(6) | 0.9765(6) | 0.0613(17) |
| C23 | 0.2242(10) | 1.7957(6) | 1.0783(5) | 0.0638(17) |
| C24 | 0.1127(11) | 1.9407(8) | 1.0669(8) | 0.091(3) |
| C25 | 1.3586(9) | −0.6568(6) | 0.3920(5) | 0.0612(16) |
| C26 | 1.4452(8) | −0.8118(6) | 0.3807(5) | 0.0519(15) |
| C27 | 1.5456(9) | −0.8907(7) | 0.4610(5) | 0.0591(17) |
| C28 | 1.6194(8) | −1.0235(6) | 0.4504(5) | 0.0604(16) |
| C29 | 1.6050(8) | −1.0955(6) | 0.3526(5) | 0.0536(15) |
| C30 | 1.5049(9) | −1.0192(6) | 0.2700(5) | 0.0637(17) |
| C31 | 1.4279(9) | −0.8799(6) | 0.2834(5) | 0.0611(16) |
| C32 | 1.6764(9) | −1.3078(6) | 0.2492(6) | 0.0643(17) |
| C33 | 1.7890(9) | −1.4567(6) | 0.2664(6) | 0.0624(18) |
| C34 | 1.7915(11) | −1.5440(7) | 0.1673(6) | 0.085(2) |
| C35 | 1.9043(11) | −1.6916(7) | 0.1746(8) | 0.092(3) |
| N2 | 0.7734(7) | 0.5929(5) | 0.7152(4) | 0.0580(13) |
| N9 | 1.2420(8) | −0.3519(5) | 0.5292(5) | 0.0626(14) |
| O1 | 0.6273(7) | 0.8615(4) | 0.7516(4) | 0.0706(13) |
| O2 | 0.7352(7) | 0.8344(5) | 0.9207(4) | 0.0810(14) |
| O3 | 0.3230(5) | 1.4840(4) | 0.8934(4) | 0.0629(12) |
| O4 | 1.3795(7) | −0.6112(5) | 0.4911(4) | 0.0768(14) |
| O5 | 1.6880(6) | −1.2331(4) | 0.3483(4) | 0.0672(13) |
| O6 | 1.2814(8) | −0.5853(5) | 0.3231(5) | 0.0893(15) |

**Table 3.** Bond lengths [A°] of non-hydrogen atoms (e.s.d's are given in parenthesis)

| Atoms | Bond length [A°] | Atoms | Bond length [A°] |
|---|---|---|---|
| C(6)-C(7) | 1.316(3) | C(6)-C(3) | 1.489(7) |
| C(15)-C(16) | 1.360(7) | C(15)-C(20) | 1.374(8) |
| C(15)-C(14) | 1.470(7) | C(26)-C(27) | 1.388(8) |
| C(26)-C(31) | 1.399(7) | C(26)-C(25) | 1.511(8) |
| C(4)-C(3) | 1.343(9) | C(4)-C(5) | 1.384(7) |
| C(29)-O(5) | 1.350(6) | C(29)-C(30) | 1.397(8) |
| C(29)-C(28) | 1.419(7) | C(8)-C(9) | 1.376(8) |
| C(8)-C(13) | 1.411(8) | C(8)-C(7) | 1.441(7) |
| N(9)-C(5) | 1.329(8) | N(9)-C(1) | 1.327(9) |
| O(3)-C(18) | 1.382(5) | O(3)-C(21) | 1.428(7) |
| C(2)-C(3) | 1.387(9) | C(2)-C(1) | 1.413(8) |
| C(25)-O(6) | 1.166(8) | C(25)-O(4) | 1.322(8) |
| C(17)-C(18) | 1.360(8) | C(17)-C(16) | 1.400(7) |
| C(18)-C(19) | 1.348(7) | C(27)-C(28) | 1.295(8) |
| C(19)-C(20) | 1.438(7) | C(31)-C(30) | 1.362(8) |
| C(32)-O(5) | 1.441(7) | C(32)-C(33) | 1.538(8) |
| C(10)-N(2) | 1.311(8) | C(10)-C(9) | 1.347(7) |
| O(1)-C(14) | 1.309(7) | C(22)-C(21) | 1.480(8) |
| C(22)-C(23) | 1.526(7) | N(2)-C(12) | 1.331(8) |
| O(2)-C(14) | 1.241(7) | C(23)-C(24) | 1.497(9) |
| C(12)-C(13) | 1.372 | C(33)-C(34) | 1.489(9) |
| C(34)-C(35) | 1.520(9) | | |



### *3.2 FTIR Studies*

It is well documented that in the infra red spectra the free alkoxy benzoic acid displays two sharp bands at 1685 and 1695 $cm^{-1}$, due to the carbonyl and a strong intense band at $\upsilon_{max}$ 3032 $cm^{-1}$ due to hydroxyl of carboxylic acid group [20]. From this, it is also concluded that the carboxylic acid exists as a dimer at room temperature. The IR spectra of the complex (Fig. 3), recorded in the solid state (KBr) at room temperature, exhibits characteristic absorption bands at $\upsilon_{max}$ 3437 (carboxylic O—H), 2948 (C—H stretching), 2871(H—N: hydrogen bond), 2376 (C=N of the pyridine ring), 1695 (conjugated C=O) and 1597, 1518, and 1243 (CH=CH) $cm^{-1}$, in addition to the other expected aromatic absorption bands. The appearance of sharp bands corresponding to carboxylic O—H and H—N hydrogen bond substantiates the observation, initially gathered from POM, DSC, and DTA studies, that the complex 3 results due to the formation of hydrogen bond between BOBA (donor) and DPE (acceptor) moieties.

### *3.3. XRD Studies*

The structure as also the presence of intermolecular hydrogen bonding in the complex 3 was further confirmed by XRD studies. An ORTEP view of the complex with atomic labeling is represented in Fig. 4. The crystal data and other experimental details are shown in Table 1.

**Table 4.** Bond angles of non-hydrogen atoms (e.s.d's are given in parentheses)

| Atoms | Bond angle [°] | Atoms | Bond angle [°] |
|---|---|---|---|
| C(7)-C(6)-C(3) | 125.0(4) | C(16)-C(15)-C(20) | 118.9(4) |
| C(16)-C(15)-C(14) | 121.3(5) | C(20)-C(15)-C(14) | 119.7(5) |
| C(27)-C(26)-C(31) | 117.4(5) | C(27)-C(26)-C(25) | 123.5(5) |
| C(31)-C(26)-C(25) | 119.1(5) | C(3)-C(4)-C(5) | 120.9(5) |
| O(5)-C(29)-C(30) | 125.7(5) | O(5)-C(29)-C(28) | 116.8(5) |
| C(30)-C(29)-C(28) | 117.5(5) | C(9)-C(8)-C(13) | 115.4(5) |
| C(9)-C(8)-C(7) | 123.1(5) | C(13)-C(8)-C(7) | 121.5(5) |
| C(5)-N(9)-C(1) | 115.3(6) | C(18)-O(3)-C(21) | 119.4(4) |
| C(3)-C(2)-C(1) | 117.7(6) | O(6)-C(25)-O(4) | 123.5(6) |
| O(6)-C(25)-C(26) | 124.9(6) | O(4)-C(25)-C(26) | 111.7(5) |
| C(18)-C(17)-C(16) | 119.3(4) | C(19)-C(18)-C(17) | 121.4(4) |
| C(19)-C(18)-O(3) | 113.8(5) | C(17)-C(18)-O(3) | 124.7(5) |
| C(28)-C(27)-C(26) | 123.0(5) | C(18)-C(19)-C(20) | 119.0(5) |
| C(30)-C(31)-C(26) | 120.7(6) | O(5)-C(32)-C(33) | 105.7(5) |
| N(2)-C(10)-C(9) | 122.4(5) | C(6)-C(7)-C(8) | 128.0(4) |
| C(21)-C(22)-C(23) | 112.7(5) | C(29)-O(5)-C(32) | 117.7(5) |
| C(15)-C(16)-C(17) | 121.4(5) | C(10)-N(2)-C(12) | 119.0(5) |
| C(27)-C(28)-C(29) | 121.0(6) | C(15)-C(20)-C(19) | 119.9(5) |
| N(9)-C(5)-C(4) | 123.8(5) | C(24)-C(23)-C(22) | 112.9(6) |
| C(4)- C(3)- C(2) | 117.7(5) | C(4)-C(3)-C(6) | 125.7(6) |
| C(2)-C(3)-C(6) | 116.6(6) | O(3)-C(21)-C(22) | 109.0(5) |
| N(2)-C(12)-C(13) | 122.0(6) | C(10)-C(9)-C(8) | 121.7(5) |
| O(2)-C(14)-O(1) | 123.0(5) | O(2)-C(14)-C(15) | 123.0(5) |
| O(1)-C(14)-C(15) | 113.9(5) | C(34)-C(33)-C(32) | 111.0(6) |
| C(31)-C(30)-C(29) | 120.3(5) | C(12)-C(13)-C(8) | 119.5(6) |
| C(33)-C(34)-C(35) | 115.0(7) | N(9)-C(1)-C(2) | 124.6(7) |

The position and displacement parameters (without hydrogen atoms) are given in Table 2, while the bond lengths and bond angles are shown in Tables 3 and 4, respectively.

The dihedral angle between the two pyridine rings is 0.87(2)°. The benzene ring in both the molecules is coplanar with the carboxyl group. In the crystal structure, the intermolecular O—H—N hydrogen bond links the molecule into chains. The packing of the molecule in the unit cell viewed down the "a" axis is shown in Fig. 5. From the crystal packing, it is seen that strong O—H—N (i.e., donor-acceptor) intermolecular interactions are responsible for the stability of the molecule in the unit cell. It is also evident from

**Table 5.** Hydrogen-bonding geometry (e.s.d's in parentheses)

| D–H . . . A | D–H [Å] | H . . . A [Å] | D . . . A [Å] | D–H . . . A [°] |
|---|---|---|---|---|
| O(1)-H(1) . . . ..N(2)[(i)] | 0.82 | 1.83 | 2.644(6) | 170 |

(i) Symmetry code: $1 + x, -1 + y, z$.

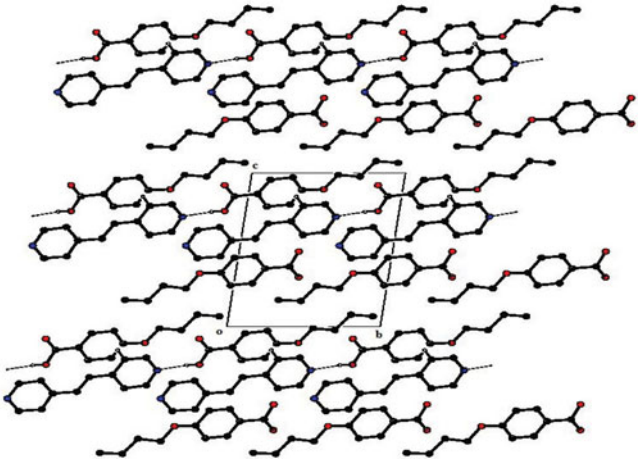

**Figure 5.** Packing arrangement of the complex viewed down the "a" axis. Hydrogen atoms are shown as small spheres of arbitrary radii.

Table 5 of hydrogen bonding geometry that a large angle of the magnitude of 170º between O—H—N (D—H—A) is possible only due to the formation of hydrogen bond in the complex.

## 4. Conclusion

A hydrogen-bonded complex between BOBA and DPE has been investigated using POM, DSC, and TA studies. The complex shows, in addition to nematic phase, smectic A phase using 1:1 mole ratio of individual components. The complex is quite stable as is envisaged by thermal gravimetric analysis that records the total loss as only 11.2% even beyond its isotropic point. The existence of the hydrogen bonded complex is confirmed using FTIR and X-ray studies. The single crystal X-ray studies also demonstrate the packing mode in the complex.

## Acknowledgments

The authors are thankful to the late Prof. T. K. Razdan, Department of Chemistry, University of Jammu, Jammu, for fruitful discussions and criticism during the course of study.

## Funding

R. K. B. is also thankful to the University Grants Commission, New Delhi, India for financial support.

## References

[1] (a) Etter M. C. (1990). *Acc. Chem. Res.*, *23*, 120. (b) Whiteslides, G. M., Mathias, J. P., & Seto, C. T. (1991), *Science*, *254*, 1312.
[2] Llamas-Saiz, A. L., Foces-Foces, C., Mo, O., Yanez, M., & Elguero, J. (1992). *Acta Cryst. B*, *48*, 700.
[3] Simard, M., Su, D., & Wuest, J. D. (1991). *J. Am. Chem. Soc.*, *113*, 4696.

[4] Aakeroy, C. B., & Seddon, K. R. (1993). *Chem. Soc. Rev.*, *22*, 397.
[5] Lehan, J. M. (1988). *Angew. Chem. Int. ed. Eng.*, *27*, 89.
[6] Constantinos, M. P., & Dimitris, T. (2001). *Liq. Cryst.*, *28*, 1127.
[7] Wei, Q. et al. (2007). *Liq. Cryst.*, *34*, 855.
[8] Benedicte, F., David, B., & Kimberley, W. (2000). *Liq. Cryst.*, *27*, 605.
[9] Lee, J. W., Jin, J. I., Archard, M. F., & Hardouin, F. (2003). *Liq. Cryst.*, *30*, 1193.
[10] Lee, J. H. et al. (2005). *Tetrahed. Lett.*, *46*, 7143.
[11] Xu, J. W., Toh, C. L., & Liu, X. (2005) *Macromolecules*, *38*, 1684.
[12] Vijaykumar, V. N., Murugadass, K., & MadhuMohan, M. L. N. (2010). *Mol. Cryst. Liq. Cryst.*, *517*, 43.
[13] Bradfield, A. E., Jones, B., & Ray, J. N. (1929). *J. Chem. Soc.*, 2660.
[14] Gray, G. W., & Jones, B. (1953). *J. Chem. Soc.*, 4179.
[15] Kato, T., & Frechet, J. M. J. (1989). *J. Am. Chem. Soc.*, *111*, 8533.
[16] Bernhardt, H., Weissflog, W., & Kresse, H. (1997). *Chem. Lett.*, 151.
[17] Kohlmeier, A., & Janietz, D. (2007). *Liq. Cryst.*, *34*, 65.
[18] Sheldrick, G. M. (2008). *Acta Cryst., A64*, 112.
[19] Demus, D., & Richter, L. (1978). *Textures of Liquid Crystals*, VEB Deutscher verlag fur grundstoffindustrie: Leipzig.
[20] Nakamoto, K. (1978). *Infrared and Raman Spectra of Inorganic and Co-ordination Compounds*, Interscience: New York.